

# Isothermal Crystallization of Random Ethylene–Butene Copolymers: Bimodal Kinetics

Buckley Crist\* and Elizabeth S. Claudio†

Department of Materials Science and Engineering and Materials Research Center,  
Northwestern University, Evanston, Illinois 60208

Received July 13, 1999; Revised Manuscript Received October 19, 1999

**ABSTRACT:** Random copolymers of ethylene and butene contain crystallizable sequences of different length  $l$ . Isothermal crystallization of model ethylene–butene random copolymers having 21 and 73 branches per 1000 backbone carbon atoms was studied by differential scanning calorimetry (DSC). Two melting peaks, which correspond to two crystal populations, are seen after isothermal crystallization. High-temperature melting is attributed to lamellar crystals formed from the longest sequences in the copolymer. These thicken during crystallization and melt at temperatures as large as 22 °C above the crystallization temperature  $T_c$ . A second crystal population melts around  $T_c + 5$  °C. It is concluded that these crystals are dominated by shorter sequences that solidify with little or no folding and hence resemble fringed micelles. Thickening is suppressed in this set of crystals, so they melt near  $T_c$ . Low melting crystals are shown to grow more slowly than the lamellar structures; the difference in transformation rates is attributed to lower undercooling and restricted mass transport for crystallization of short sequences. No comparable evidence for two crystal populations is seen when unbranched polyethylene or a heterogeneous copolymer (19 branches/1000 C) is crystallized isothermally under similar conditions.

## Introduction

We recently reported on the crystallization and melting of model ethylene–butene random copolymers.<sup>1</sup> Melting after isothermal crystallization led, surprisingly, to two well-defined maxima in the differential scanning calorimetry (DSC) endotherm above the crystallization temperature  $T_c$ . All the copolymers considered, with branch concentrations from 21 to 106 ethyl branches/1000 backbone C atoms, displayed what appears to be two crystal populations after isothermal crystallization. It should be emphasized that these copolymers are compositionally uniform, with all chains having the same concentration of ethyl branches.

While isothermal crystallization experiments on random copolymers are not common, similar or related observations have been made by others. The first such study was done on random copolymers of ethylene and vinyl acetate by Okui and Kawai,<sup>2</sup> who observed two melting peaks above the isothermal crystallization temperature  $T_c$ . These features were unaffected by heating rate, so melting, recrystallization, and remelting (mrr) were not responsible. In subsequent work it was reported that the high-temperature endotherm appeared first.<sup>3</sup> Two DSC endothermic peaks seen by Maderek and Strobl<sup>4</sup> for high-pressure polyethylene containing 24 branches/1000 C were ascribed without proof to mrr. Alamo and Mandelkern<sup>5</sup> considered isothermally crystallized ethylene–butene copolymers. Here only one peak was seen above  $T_c = 100$  °C, and mrr was dismissed due to the lack of effect of heating rate on endotherms of quench crystallized copolymers. Schouterden et al.<sup>6</sup> saw two clearly resolved melting peaks above the nominal crystallization temperature  $T_c = 105$  °C for an ethylene–octene copolymer (10 branches/1000 C). This copolymer is heterogeneous, with the

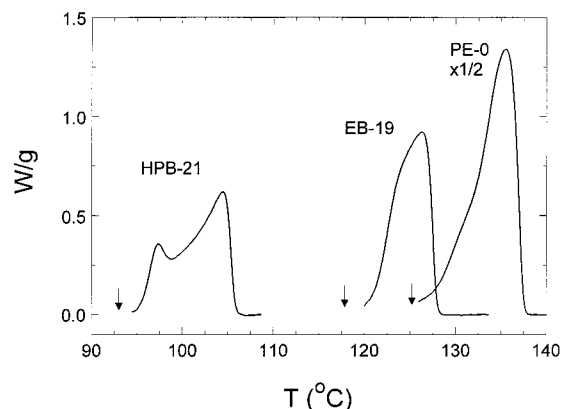
amount of short chain branching varying substantially from chain to chain. No explanation was given for the two melting peaks, but it is likely that the least branched chains crystallized during cooling to  $T_c = 105$  °C. Homogeneous copolymers prepared with metallocene catalysts have been the subject of more recent work. Kim and Phillips<sup>7</sup> considered ethylene–octene and ethylene–butene copolymers after isothermal crystallization for 1 day or longer. A single endotherm with peak temperature  $T_m^p$  about 5 °C above  $T_c$  was observed, and crystallization appeared to continue for months. Androsch<sup>8</sup> examined an ethylene–octene copolymer having 37 branches/1000 C. Primary crystallization occurred on quenching to room temperature, and storage at room temperature led to additional “secondary” crystallization, during which a low-temperature endotherm grew in magnitude and  $T_m^p$ . A series of ethylene–octene copolymers were investigated by Alizadeh et al.,<sup>9</sup> who extended the room temperature aging experiments of Androsch. They also isothermally crystallized chains having 62 hexyl branches/1000 C, after which two endotherms are observed above  $T_c > 40$  °C. Random syndiotactic poly(propylene-*co*-octene), 8.5 and 32 octene/1000 C, were isothermally crystallized by Hauser et al.<sup>10</sup> The low octene copolymer shows clear evidence of mrr when heated. Melting of isothermally crystallized high octene copolymer occurs over a broad range, but endothermic activity at relatively low temperatures appears to increase with crystallization time.

In this paper we present additional results for isothermally crystallized random copolymers. It is shown that two melting peaks are seen after isothermal crystallization of homogeneous copolymers, not heterogeneous copolymers or homopolymers. The issue of melting, recrystallization, and remelting (mrr) is addressed. Kinetic studies show that crystals that melt at the lower temperature are formed more slowly than those melting at higher temperatures.

† Present address: Department of Chemistry, Northwestern University, Evanston, IL 60208.

Table 1. Characteristics of Polymers

polymer	br/1000 C <sup>a</sup>	$M_w$ (kg/mol)	$M_w/M_n$
PE-0	0	119	1.2
EB-19	19.4	130	4.2
HPB-21	21	96	<1.1
HPB-73	73	186	<1.1

<sup>a</sup> Ethyl branches per 1000 backbone C atoms.

**Figure 1.** DSC scans of melting of isothermally crystallized HPB-21 ( $T_c = 93$  °C), EB-19 ( $T_c = 118$  °C), and PE-0 ( $T_c = 125.4$  °C). Heating was at 5 °C/min directly following crystallization at temperatures indicated by arrows.

## Experimental Section

The model ethylene–butene random copolymers used here are HPB-21 and HPB-73. These are hydrogenated polybutadienes, the synthesis and characterization of which have been reported previously.<sup>11,12</sup> A conventional (heterogeneous) ethylene–butene copolymer<sup>13</sup> is designated EB-19, and unbranched polyethylene PE-0 is a fractionated reference material from NIST. The numerical suffix is the number of ethyl branches per 1000 backbone C atoms; chemical characteristics are given in Table 1.

Calorimetry was done with a Perkin-Elmer DSC 7 calibrated with indium and gallium or tin. PE-0, HPB-21, and EB-19 (sample mass of 3.8–4.9 mg) were treated in a like manner. Molten polymer was cooled at  $-50$  °C/min from 165 °C to the isothermal crystallization temperature  $T_c$  that was chosen so the maximum crystallization rate occurred at about 5 min. After 15–20 min at  $T_c$ , crystallization was sensibly complete, and the polymer was heated at 5 °C/min unless stated otherwise. For heating rate studies, HPB-21 was also melted at 2.5 and 10 °C/min, both directly after crystallization and after an intermediate cooling step ( $-50$  °C/min) to 30 °C. HPB-73 was the subject of crystallization rate studies. The 7.7 mg sample was crystallized at 48 and 50 °C for various times and then heated at 5 °C/min. Temperature calibration was adjusted for heating rate, but exotherm distortion due to thermal lag<sup>14</sup> was ignored, which is reasonable for scan rates of 10 °C/min or less.

It should be noted that undercoolings to achieve similar normalized crystallization rates are about 20 °C for PE-0, 45 °C for HPB-21, and 70 °C for HPB-73. These are dictated primarily by branching and secondarily by molecular weight. It is impossible to crystallize copolymers with strongly different compositions at the same undercooling.

## Results

Endotherms for isothermally crystallized PE-0, EB-19, and HPB-21 are shown in Figure 1. Crystallization temperatures, peak melting temperatures, and heat of fusion are given in Table 2. Melting endotherms of the unbranched PE-0 and heterogeneously branched EB-19 are qualitatively similar, being skewed to low temperatures and terminating at a final melting tempera-

Table 2. Isothermal Crystallization of Polymers

polymer	$T_c$ (°C)	$T_m^p$ (°C) <sup>a</sup>	$\Delta H_m$ (J/g)
PE-0	125.4	135.5	151
EB-19	118	126	46
HPB-21	93	97.5, 104.5	44
HPB-73	48	52.9, (59), 63.6	8.8
HPB-73	50	55.1, 65.3	7.0

<sup>a</sup> From DSC scans at 5 °C/min.

ture  $T_m^f$  about 10–12 °C greater than  $T_c$ . Note the virtual lack of endothermic activity in the 5 °C range above  $T_c$ . It is well established that polyethylene crystals thicken during isothermal crystallization,<sup>15</sup> shifting the melting range upward. What appear as shoulders on the low-temperature sides of the endotherms may imply that thickening is incomplete in the ca. 20 min allowed for crystallization. Temperature rising elution fractionation (TREF) shows that about 30% of the chains EB-19 have a branch content of 3/1000 C.<sup>13</sup> These lightly branched chains crystallize quite similarly to the unbranched molecules in PE-0, although melting temperature is lowered because crystal thickness is reduced somewhat by excluded ethyl branches and by the presence of branches in the coexisting melt.<sup>16,17</sup>

HPB-21, a homogeneous copolymer, displays two well-resolved maxima in the endotherm following isothermal crystallization. The melting region extends to 13 °C above  $T_c$ , a point of similarity to PE-0 and EB-19. But a significant difference is the presence of a low-temperature peak located about 5 °C above  $T_c$ . A sizable fraction of crystals in HPB-21 melt just above the crystallization temperature, which is not the case for the homopolymer or the heterogeneous copolymer. Recall that crystallization rates and times are similar for all three cases. Below is developed the thesis that low melting crystals are those that do not thicken during isothermal crystallization. We note in passing that melting in HPB-21 occurs more than 20 °C below that for EB-19, which has a similar average ethyl branch content. Isothermal crystallization at  $T_c \approx 118$  °C fractionates the heterogeneous EB-19 copolymer by solidifying only the plentiful lightly branched chains. Such molecular fractionation cannot occur with homogeneous HPB-21 chains at any  $T_c$ . The fact that heats of melting (Table 2) are similar for HPB-21 and EB-19 is thought to be coincidental.

Branch exclusion leads to the formation of relatively thin crystals in homogeneous copolymers such as HPB. It is well established that thin homopolymer crystals can melt, recrystallize at large undercoolings, and remelt (mrr) during heating.<sup>18</sup> Heating rate was varied to examine this as the possible cause of two peaks in HPB-21. One should appreciate that DSC transients, which are more severe for larger heating rates, interfere with the observation of melting at the beginning of a scan. For this reason data in Figure 1 are missing just above  $T_c$  in the two low crystallinity copolymers. To eliminate transients in the temperature range of interest, isothermally crystallized HPB-21 was cooled to 30 °C before heating at 2.5, 5, or 10 °C/min as shown in Figure 2. The lowest temperature feature is for that part of the copolymer that crystallized on cooling to 30 °C. Focusing on the region of interest above  $T_c = 93$  °C, the low-temperature portion of the endotherm around  $T = 97$  °C is rate-dependent in a manner that suggests melting and recrystallization. Specifically, recrystallization at the slowest rate of 2.5 °C/min is likely

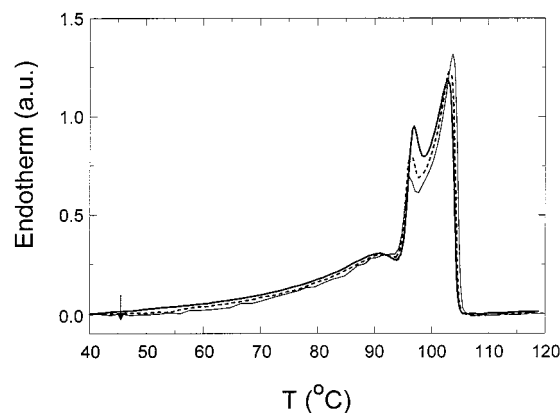


**Figure 2.** DSC scans for HPB-21 crystallized at  $T_c = 93$  °C for 20 min and then cooled to 30 °C at 50 °C/min. Heating rates are 2.5 °C/min (thin line), 5 °C/min (dashed line), and 10 °C/min (thick line).

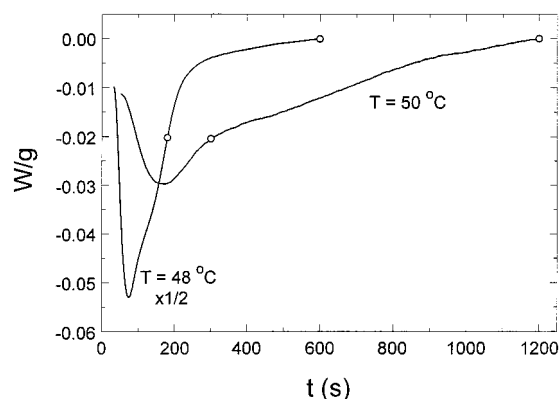


**Figure 3.** Exotherm during isothermal crystallization of HPB-73 at 50 and 48 °C. Open points indicate times at which crystallization was terminated for kinetic studies.

responsible for the decrease in the height of the low-temperature peak and for the smaller magnitude of the endotherm between the two peaks. Remelting of the recrystallized segments and annealing (for the 2.5 °C/min scan, the endotherm width corresponds to 5 min at temperatures above  $T_c$ ) are consistent with the increased size and temperature of the high-temperature peak. The heat of melting above  $T_c = 93$  °C is constant (within 4%) for the three rates, as expected. Basically the same results, confounded by transients that affect data just above  $T_c = 93$  °C, were obtained by heating directly without cooling to 30 °C. These observations lead to the question: Is the high-temperature peak the product of remelting alone? If the answer is “yes”, then two peaks do not signify two crystal populations.

Additional information on this issue can be obtained from the relative rates at which the low- and high-temperature peaks evolve at  $T_c$ . HPB-73 was selected for these experiments because of some interesting features shown in Figure 3. As pointed out in an earlier study,<sup>1</sup> this highly branched copolymer gives calorimetric evidence of crystallizing in two stages. For  $T_c = 50$  °C, there is a maximum heat evolution at  $t_{\max} = 170$  s and a shoulder at 470 s suggesting a slower mechanism. Decreasing the crystallization temperature by 2 °C shifts these times to 80 and 150 s, respectively. Notice also that crystallization persists for times longer than  $7t_{\max}$ . In contrast, isothermal crystallization of PE-0, EB-19, or HPB-21 leads to an exotherm that is nearly

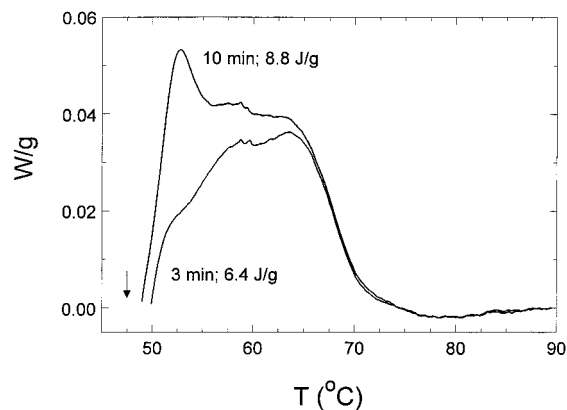


**Figure 4.** DSC curve for melting HPB-73 after crystallization at  $T_c = 48$  °C for 3 and 10 min.

symmetric about  $t_{\max}$ , with crystallization apparently completed by  $2.5t_{\max}$ .

HPB-73 was crystallized for 3 and 10 min at  $T_c = 48$  °C and for 5 and 20 min at  $T_c = 50$  °C; these times are indicated by open points in Figure 3. The sample was heated at 5 °C/min to observe melting of crystals formed during the corresponding time at  $T_c$ . In this experiment one must realize that crystallization is incomplete after the allotted interval and continues for a finite time when the sample is heated above  $T_c$ . The “residual” heat of crystallization interferes with the observation of melting at temperatures close to  $T_c$  (in addition to DSC transients), so times greater than  $t_{\max}$  were selected to reduce such interference. Results for HPB-73 crystallized at 48 °C are presented in Figure 4. The lowest temperature peak at 53 °C appears as a shoulder after 3 min and grows to a well-defined maximum after 10 min. This establishes unambiguously that those crystals that melt at high temperatures form first (within 3 min) and that the majority of the low melting crystals develop in the latter stages of the transformation. Note that residual crystallization limits the range of observable low-temperature melting for the 3 min sample. An estimate of the consequence can be made by comparing heats of crystallization at the two times to the respective heats of melting. The melting endotherm for the 3 min sample is deficient by 0.6 J/g, or less than 10% of the area. So the low-temperature region in this experiment is under-represented in Figure 4, but by a small amount that does not change the conclusion that high melting crystals form first. A important corollary is that high-temperature melting, which is the same after 3 and 10 min, is not an artifact due to mrr. Hence, high- and low-temperature melting peaks indeed signify the presence of two crystal populations. Similar results and conclusions were reported for isothermally crystallized ethylene–vinyl acetate copolymers<sup>3</sup> and for quenched and aged ethylene–octene copolymers.<sup>9</sup>

To explore still earlier stages of crystallization,  $T_c$  was raised to 50 °C to slow the overall transformation by slightly more than 50%. Here the short crystallization time of 5 min (300 s) is before the shoulder in Figure 3. Results in Figure 5 again support the notion that high  $T_m^p = 65$  °C crystals grow first, followed by crystals that melt at  $T_m^p = 55$  °C. After 5 min there is no evidence of the low-temperature peak, which confirms the premise that low melting crystals are associated with the slow thermal process centered near 470 s in Figure 3. Data summarized in Table 2 show that both low and high



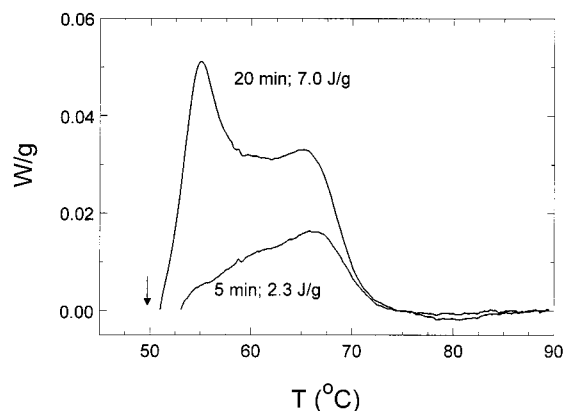


**Figure 5.** DSC curve for melting HPB-73 after crystallization at  $T_c = 50$  °C for 5 and 20 min.

peak melting temperatures increase by about 2 °C when  $T_c$  is raised from 48 to 50 °C. Following crystallization at 48 °C there is an intermediate endotherm feature at 59 °C, which is absent at the higher crystallization temperature. It is not known whether this represents yet a third crystal population or follows from some subtle mrr effects.

The same delayed appearance of the low-temperature melting peak is likewise seen with HPB-21 during crystallization at  $T_c \approx 93$  °C. As mentioned above, the crystallization exotherm gives no evidence for resolved fast and slow transformation processes, but this is attributed to the relatively small portion of segments forming low melting crystals. Note in Figure 1 that the contribution of the low-temperature peak to the total endotherm for HPB-21 is much smaller than that for HPB-73. Given the kinetic evidence, we believe that the mrr effects observed at different scan rates in Figure 2 are real but of no fundamental importance. A portion of the least stable crystals, which melt closest to  $T_c$ , recrystallize and contribute to the high-temperature peak, but high-temperature melting is seen in the presence of little or no low-temperature melting (see Figures 4 and 5). The significant point is that a bimodal crystal population is created during isothermal crystallization of homogeneous random copolymers.

## Discussion

A model for the formation of two crystal populations in random copolymers was presented recently by Crist and Williams.<sup>1</sup> The model starts with the length distribution of crystallizable, in this case ethylene, sequences present in the copolymer. At any given crystallization temperature  $T_c$ , molten sequences longer than some length  $l^*$  are undercooled and can participate in crystallization. Assuming lamellar crystals of thickness  $l^*$  with basal surface energy  $\sigma_e$ , the relevant expression is<sup>1,17</sup>

$$l^* = \frac{2\sigma_e}{\Delta H_v} \frac{T_m^c}{T_m^c - T_c} \quad (1)$$

Here the heat of fusion per unit volume of crystalline polyethylene is  $\Delta H_v$ , and  $T_m^c$  is the thermodynamic melting point for a random copolymer with mole fraction  $x_e$  of crystallizable (ethylene) repeat units.<sup>16</sup>

$$\frac{1}{T_m^c} = \frac{1}{T_m^0} - \frac{R}{\Delta H_u} \ln x_e \quad (2)$$

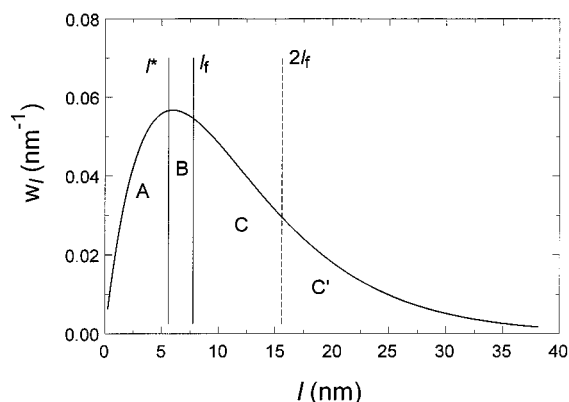


**Figure 6.** Distribution of ethylene sequence lengths in HPB-21. The vertical line separating A and B is from eq 1, and that separating B from C is from eq 3. See text for significance of regions A, B, and C and C'.

In eq 2,  $T_m^0$  is the equilibrium melting point of a perfect (infinitely thick) polyethylene crystal, and  $\Delta H_u$  is the heat of fusion per mole of crystalline (ethylene) units. Equation 1 can be recognized as the Gibbs–Thompson relation for melting lamellar crystals wherein  $T_m^0$  has been replaced by  $T_m^c$ . With standard thermodynamic values for polyethylene crystals<sup>19,20</sup> ( $T_m^0 = 418.7$  K,  $\sigma_e = 90$  mJ/m<sup>2</sup>,  $\Delta H_v = 285$  mJ/m<sup>3</sup>), results for HPB-21 (random copolymer with ethylene mole fraction  $x_e = 0.96$ ) are  $T_m^c = 138$  °C, and  $l^* = 5.6$  nm at  $T_c = 93$  °C.

A second length is established by the final melting temperature  $T_m^f$  of crystals grown at  $T_c$ . While we lack a kinetic theory to account for actual crystallization of random copolymers, the largest thickness of crystals present can be obtained from the final melting temperature, which is  $T_m^f = 106$  °C for HPB-21. This temperature corresponds to equilibrium between the melt with overall ethylene concentration  $x_e = 0.96$  and lamellar crystals of thickness  $l_f$ .<sup>1,17</sup>

$$l_f = \frac{2\sigma_e}{\Delta H_v} \frac{T_m^c}{T_m^c - T_m^f} \quad (3)$$

From eq 3 we establish the upper limit of crystal thicknesses formed at  $T_c = 93$  °C is  $l_f = 7.8$  nm.

Figure 6 depicts the weight fraction  $w_l$  of ethylene sequences of different lengths  $l$  in HPB-21, calculated on the assumption that the polymer is a random copolymer with ethylene mole fraction  $x_e = 0.96$ .<sup>17</sup> Crystal thicknesses are constrained between the vertical lines marking  $l^* = 5.6$  nm and  $l_f = 7.8$  nm; this range B is narrow compared to the distribution of sequence lengths. Region A is for sequences too short to be incorporated in stable crystals at 93 °C. The balance, which comprises 70 wt % of the copolymer, can participate in crystals that are expected to be somewhat thicker than  $l^* = 5.6$  nm. These sequences with  $l > l^*$  can be sorted into two categories regarding crystallization. The shortest ones in regions B and C, with  $l \lesssim 2l_f$  (about 16 nm), must solidify as extended sequences without incorporating ethyl branches in the crystal. Sequences longer than  $2l_f \approx 16$  nm, region C', may fold at least once during the crystallization of lamellae with thickness between  $l^*$  and  $l_f$ . Hence, the distribution of undercooled sequence lengths in a molten random copolymer sets the stage for two types of crystallization behavior.

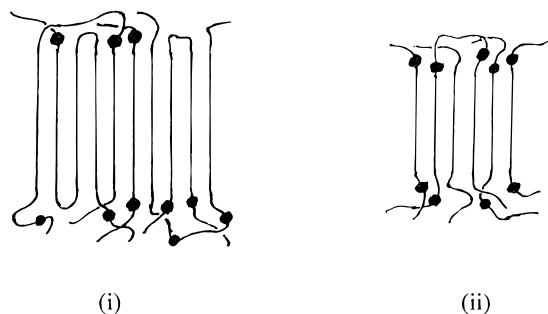


**Figure 7.** Schematic representations of (i) lamellar crystals formed by long segments in regions C and C' and (ii) fringed micelles composed largely by shorter segments from region B. Short chain branches are represented by ●.

Additional features are implicit in the distribution function  $w_l$ . The most evident is that the concentration of long C' sequences is small, with the suggestion that these would make correspondingly meager contributions to crystal growth. However, we borrow from Flory<sup>16</sup> the idea that long sequences are more undercooled than short sequences at a particular  $T_c$ , because the entropy of fusion includes a term for mixing comonomers in the melt state, which is obviously larger for the melting of shorter sequences. Indeed, the undercooling of sequences with  $l = l^*$  is zero. Anticipating that kinetic factors will favor the growth of crystals with  $l \approx l^*$  (5.6 nm in Figure 6), long sequences with  $l > 16$  nm are expected to contribute to crystallization in excess of their small concentration because larger undercooling results in faster crystallization. Transport effects work in the same direction as this thermodynamic argument. A long sequence can attach to the growth face in a relatively unencumbered manner, whereas acceptable sorption of a short sequence, particularly one in region B, is more difficult because both branch points must be excluded from the substrate.

Having established this background, the origin of two crystal populations becomes evident. Molten HPB-21 at  $T_c = 93$  °C has 70% of the copolymer as undercooled sequences with  $l > l^* = 5.6$  nm, which have been subdivided into regions B (13%), C (32%), and C' (25%). Consider first those sequences in regions C and C', which constitute over half of the material. Such sequences can form lamellar crystals of thickness  $l \lesssim l_f$  with appreciable folding of the longest C' sequences, while intermediate C sequences participate as extended sequences with chain folding (as opposed to sequence folding) as sketched in Figure 7i. Be reminded that a crystallized stem may be a fraction of the sequence length. The crystallization process just described is closely related to that in homopolymers. One difference is that only slightly more than half of the copolymer is eligible to crystallize in this manner. Furthermore, folding is constrained by ethyl branches but is adequate to permit the formation of lamellar crystals as shown by electron microscopy<sup>21</sup> and small-angle X-ray patterns,<sup>12</sup> observations that clearly refute Flory's early contention to the contrary.<sup>22</sup> Lamellar crystals developed in this conventional manner give rise to the high-temperature melting peak with  $T_m^p = 105$  °C and  $T_m^f = 106$  °C. We reiterate that the final melting temperature  $T_m^f$  is 13 °C above  $T_c$ , with the implication that thickening during growth is similar to that in polyethylene homopolymer. All these effects support the use of  $\sigma_e = 90$  mJ/m<sup>2</sup> to establish  $l_f$  in eq 3.<sup>1</sup> A final point is that not all of the C and C' sequences crystallize; the

heat of melting in Table 2 corresponds to a crystalline fraction of about 0.15 ( $\Delta H_f = 296$  J/g for polyethylene crystals<sup>19</sup>), or less than one-third of the C and C' sequences in HPB-21.

Low-temperature melting is from crystals dominated by the shorter undercooled sequences in region B. These must solidify as extended sequences, but adjacent chain folding is possible when B sequences are near neighbors along the chain. It is likely that some longer sequences (regions C and C') also participate in these thinner crystals, but thickness is limited by the preponderance of shorter sequences. A small population of longer sequences in the low melting crystals is the likely cause of the modest mrr effect in Figure 2. The possibility of adjacent or near-adjacent reentry is very low in these structures, which are represented in Figure 7ii as fringed micelles. Melting temperature is lower ( $T_m^p = 98$  °C) because the crystals are thinner, and they may also have a larger basal surface energy  $\sigma_e$  and lateral surfaces with energy  $\sigma$  that further lower  $T_m$ .

Hence, the sequence length distribution leads to two crystal populations in a random copolymer that melt at different temperatures. The longer sequences in regions C and C' are incorporated into lamellar crystals similar to those formed in the homopolymer, while the shorter sequences (region B) are confined to thinner crystals which, because of limited folding, are more like fringed micelles. It should be understood that the situation sketched in Figure 6 represents a model, not a theory. The relation between sequence distribution  $w_l$  and critical length  $l^*$  (established by  $T_c$ ) is indeed based on first principles. However, the important length  $l_f$  is from the final melting temperature  $T_m^f$  of crystals formed irreversibly in a manner that we do not understand in detail. Our phenomenological approach has precedents of which we were unaware at the time of our first report.<sup>1</sup> Kilian and Fischer proposed over 30 years ago that long sequences in random copolymers would form folded sequence lamellae and that the shorter sequences would crystallize as "bundles".<sup>23</sup> Some years later, Okui and Kawai<sup>3</sup> developed a model similar in many ways to the one presented here. Their analysis uses DSC crystallinity (endotherm area) to establish the equivalent of  $2l_f$  in Figure 6. That approach assumes that high melting crystallinity is directly proportional to area C' and that lamellar crystals contain no shorter sequences from the C region. We are more comfortable with eq 3 to evaluate  $l_f$  (and hence  $2l_f$ ), as fewer assumptions are involved. The present model<sup>1</sup> and the Okui–Kawai model<sup>3</sup> both account for the observation that low-temperature melting is more dominant in more branched copolymers, although quantitative significance is compromised by the delayed appearance of the low-temperature population (Figures 4 and 5) and partial mrr effects (Figure 2).

Crystallization rate is larger for those structures, which we posit are lamellar crystals formed by longer sequences, that melt at higher temperature. Why do the less branched segments in the distribution crystallize first? Again we acknowledge that no quantitative theory for irreversible crystallization of random copolymers is available. Flory's model predicts the longest sequences to crystallize first as fringed micelles during slow (equilibrium) cooling.<sup>16</sup> Should this process start, network formation would almost immediately reduce mobility so nonequilibrium crystallization must occur at longer times or at lower temperatures.<sup>17</sup> While the idea

of topological constraints leading to delayed crystallization of highly branched sequences has been invoked by others,<sup>9</sup> we find it generally unsatisfactory. Consider the case of HPB-73 crystallized at 48 °C (Figure 4). From a plot like Figure 6, 30 wt % of the polymer is undercooled segments.<sup>1</sup> Primary crystallization appears complete in about 3 min, and the heat of melting corresponds to about 2–3% crystallinity. Having established that these high melting crystals are of the folded, lamellar type, it is difficult to envision this trivial fraction of crystals impeding the aggregation of the remaining undercooled sequences. We mentioned above that crystallization of long sequences is favored by increased undercooling and fewer impediments to attachment to the growth face. Taken together, these factors ensure that longer sequences of a molten copolymer crystallize more rapidly than shorter sequences. It is unlikely that restricted segment mobility caused by formation of the first crystal population significantly slows mass transport during the second crystallization step, at least for the experiments communicated here.

While beyond the scope of this report, it is recognized that many stiff chain homopolymers such as PEEK,<sup>24</sup> PPS,<sup>25</sup> and PTMI<sup>26</sup> (but not unbranched polyethylene) display low- and high-temperature endotherms after isothermal crystallization from the melt state. Just as in the random copolymer case, the low-temperature endotherm develops more slowly, with perhaps one exception.<sup>25</sup> Here the second, low-temperature endotherm is logically accounted for by secondary crystallization of constrained sequences generated by primary crystallization; there are no sequences based on non-crystallizable comonomers and no differences in undercooling. For the three stiff-chain polymers mentioned above, primary crystallinity is in the range 0.3–0.4, which is large enough to influence the mobility of molten chain segments.

We have asserted that the longer sequences (regions C and C' in Figure 6) crystallize similarly to homopolymers. To the extent that this is true, the first lamellar crystals are formed with a kinetically controlled thickness distribution with a mean slightly greater than  $l^*$  (termed  $l_g^*$  in the Hoffman–Lauritzen theory<sup>27</sup>), and these thicken rapidly to establish  $l_f$  as do homopolymer crystals, raising  $T_m^f$  to  $T_c + 13$  °C for HPB-21 and  $T_c + 22$  °C for HPB-73. For copolymers, however, thickening by axial diffusion of chain stems is limited by the presence of branches. This restriction is indicated by the ratio  $l_f/l^* \approx 1.4$  for HPB-21 and HPB-73,<sup>1</sup> whereas isothermal thickening in polyethylene more than doubles  $l$ .<sup>15,28</sup> Turning to the second population of copolymer crystals that have fringed micelle character, thickening is effectively suppressed by the high concentration of branch points associated with short sequences. Hence, the kinetically defined crystal thickness distribution for this portion of the copolymer is preserved until it melts about 5 °C above  $T_c$ . Note that the maximum lamellar thickness  $l_f$  (eq 3) is thermodynamically sound. One cannot, however, determine the thickness of lower melting crystals in a copolymer from  $T_m$  because the melt composition is unknown<sup>1,17,28</sup> and the crystals are not lamellar. Nevertheless, all crystals formed at  $T_c$  are thicker than  $l^*$  (eq 2).

## Conclusions

Isothermal crystallization of molten, homogeneous, random ethylene–butene copolymers results in two

melting peaks that reflect two crystal populations. A model for this observation is based on the distribution of crystallizable sequence lengths  $w_l$ . The longest sequences form crystals that melt about 10–20 °C above the crystallization temperature  $T_c$ . While folding is hindered by the presence of branches, it is nonetheless adequate to reduce the surface density of emerging crystalline stems to the point where lamellar crystals are formed, as is the case in homopolymer crystallization.<sup>22,29</sup> This fractionation of the longest sequences, which is essential to the formation of lamellar crystals, has received inadequate attention in the past. Lamellar crystals thicken during crystallization, raising the melting temperature above  $T_c$ . At later times, shorter undercooled sequences establish the second crystal population which is envisioned as being much like fringed micelles. Reduced undercooling and restrictions on transport to the growth face are responsible for sluggish kinetics for solidification of these sequences. The resulting crystals have little chain folding, and thickening is suppressed by the high concentration of branch points. Hence, the second crystal population melts about 5 °C above  $T_c$ .

Similar two-stage crystallization processes based on different sequence lengths have been proposed by Okui and Kawai<sup>3</sup> and by Alizadeh et al.<sup>9</sup> Common conclusions are that crystals that melt at the highest temperatures are lamellar, while those with lower  $T_m$  are fringed micelles. The analysis presented here relies on quantitative sequence distributions and furthermore addresses the question of why lower melting crystals do not form first. Our treatment of bimodal crystallization kinetics has no obvious relation to the spherulite completion model of Akpalu et al.,<sup>30</sup> who studied an ethylene–octene copolymer having 2 branches/1000 C atoms. It is likely that such a sparsely branched copolymer would behave as a homopolymer, as the mean sequence length is much longer than conventional lamellar thicknesses.

The relation between bimodal crystallization and sequence length distribution is confirmed by the absence of such effects in the homopolymer PE-0 and in the heterogeneous copolymer EB-19. There are no branch points in the homopolymer to define sequence lengths, and melting reflects the monomodal crystal thickness distribution established by secondary nucleation and subsequent thickening.<sup>15,31</sup> Heterogeneous copolymers have a substantial fraction of chains (as opposed to sequences) with very little branching.<sup>13</sup> For the case of EB-19, the average sequence length of the low branched chains is 85 nm, substantially larger than kinetically defined crystal thickness of ca. 15 nm. Hence, 30% of the chains in EB-19 may crystallize and thicken isothermally like the homopolymer.

We finish this report by emphasizing that the distribution of sequence lengths is critical to understanding crystallization and morphology in random copolymers. Interpretation of observations in terms of average branch concentration can be quite misleading, as evidenced by the different characteristics of HPB-21 and EB-19, which have similar overall branching.

**Acknowledgment.** This work was supported in part by the Materials Research Internship for Minority Undergraduates program with National Science Foundation funds (DMR 96-32472) administered by Northwestern's Materials Research Center.



## References and Notes

- (1) Crist, B.; Williams, D. N. *J. Macromol. Sci., Phys.* **2000**, B39, 1.
- (2) Okui, N.; Kawai, T. *Makromol. Chem.* **1972**, 154, 161.
- (3) Okui, N.; Kawai, T. *Kobunshi Ronbunshu* **1974**, 3, 1325.
- (4) Maderek, E.; Strobl, G. R. *Makromol. Chem.* **1983**, 184, 2553.
- (5) Alamo, R.; Mandelkern, L. *J. Polym. Sci., Part B: Polym. Phys.* **1986**, 24, 2087.
- (6) Schouterden, P.; Groenickx, G.; Van der Heijden, B.; Jansen, F. *Polymer* **1986**, 28, 2099.
- (7) Kim, M.-H.; Phillips, P. J. *J. Appl. Polym. Sci.* **1998**, 70, 1893.
- (8) Androsch, R. *Polymer* **1999**, 40, 2805.
- (9) Alizadeh, A.; Richardson, L.; Xu, J.; McCartney, S.; Marand, H.; Cheung, W.; Chum, S. *Macromolecules* **1999**, 32, 6221.
- (10) Hauser, G.; Schmidtke, J.; Strobl, G. *Macromolecules* **1998**, 31, 6250.
- (11) Krigas, T. M.; Carella, J. M.; Struglinski, M. J.; Crist, B.; Graessley, W. W.; Schilling, F. C. *J. Polym. Sci., Polym. Phys. Ed.* **1985**, 23, 509.
- (12) Crist, B.; Howard, P. R. *J. Polym. Sci., Part B: Polym. Phys.* **1989**, 27, 2269.
- (13) Mirabella, F. M.; Westphal, S. P.; Fernando, P. L.; Ford, E. A.; Williams, J. G. *J. Polym. Sci., Part B: Polym. Phys.* **1988**, 26, 1995.
- (14) Plummer, C. J. G.; Kausch, H.-H. *Polym. Bull.* **1996**, 36, 355.
- (15) Barham, P. J.; Keller, A. *J. Polym. Sci., Part B: Polym. Phys. Ed.* **1989**, 27, 1029.
- (16) Flory, P. J. *Trans. Faraday Soc.* **1955**, 51, 848.
- (17) Crist, B.; Howard, P. R. *Macromolecules* **1999**, 32, 3057.
- (18) Wunderlich, B. *Macromolecular Physics*; Academic Press: New York, 1980; Vol. 3, Chapter 9.
- (19) Mandelkern, L.; Alamo, R. G. In *Physical Properties of Polymers Handbook*; Mark, J. E., Ed.; American Institute of Physics: Woodbury, NY, 1996; Chapter 11.
- (20) Hoffman, J. D.; Miller, R. L. *Polymer* **1997**, 38, 3151.
- (21) Voigt-Martin, I. G.; Alamo, R.; Mandelkern, L. *J. Polym. Sci., Part B: Polym. Phys.* **1986**, 24, 1283.
- (22) Flory, P. J. *J. Am. Chem. Soc.* **1962**, 84, 2857.
- (23) Kilian, H. G.; Fischer, E. W. *Kolloid Z. Z. Polym.* **1966**, 211, 40.
- (24) Cheng, S. Z. D.; Cao, M.-Y.; Wunderlich, B. *Macromolecules* **1986**, 19, 1868.
- (25) Chung, J. S.; Cebe, P. *Polymer* **1992**, 33, 2312.
- (26) Phillips, R. A.; McKenna, J. M.; Cooper, S. L. *J. Polym. Sci., Part B: Polym. Phys.* **1994**, 32, 791. Phillips, R. A.; Cooper, S. L. *Polymer* **1994**, 35, 4146.
- (27) Hoffman, J. D.; Davis, G. T.; Lauritzen, J. I. In *Treatise on Solid State Chemistry*; Hannay, N. B., Ed.; Plenum Press: New York, 1976; Vol. 3, pp 548–553.
- (28) Crist, B.; Mirabella, F. M. *J. Polym. Sci., Part B: Polym. Phys.* **1999**, 37, 3131.
- (29) Frank, F. C. *Discuss. Faraday Soc.* **1979**, 68, 7.
- (30) Akpalu, Y.; Keilhorn, L.; Hsiao, B. S.; Stein, R. S.; Russell, T. P.; van Egmond, J.; Muthukumar, M. *Macromolecules* **1999**, 32, 765.
- (31) Barham, P. J. In *Materials Science and Technology*; Cahn, R. W., Haasen, P., Kramer, E. J., Thomas, E. L., Eds.; VCH Publishers: New York, 1993; Vol. 12; Chapter 4.

MA991131R